

TRANSPORT IN HIGH-PERFORMANCE PLASMAS OF THE TJ-II STELLARATOR: FROM FIRST-PRINCIPLES SIMULATIONS TO EXPERIMENTAL VALIDATION

¹J. M. GARCÍA-REGAÑA AND THE TJ-II TEAM

¹Laboratorio Nacional de Fusión, CIEMAT, 28040 Madrid, Spain

Email: jose.regana@ciemat.es

1. HIGH PERFORMANCE SCENARIOS IN THE OPTIMIZED STELLARATOR ERA

In stellarators and tokamaks, transport of energy, particles, and momentum in the plasma core largely determines the performance of the device. Since the advent of stellarator optimization through computational design, configurations with increasingly improved transport properties have been obtained. The largest example built to date is the Wendelstein 7-X (W7-X) stellarator, which has successfully demonstrated reduced neoclassical transport and bootstrap current as a result of this optimization approach [1]. However, the optimization of W7-X is insufficient with respect to some aspects in the path towards stellarator reactors, such as fast-ion confinement and turbulent transport. Recently, configurations with lower fast ion losses or reduced turbulent transport have been obtained, see e.g. [2-5] and references therein.

Nonetheless, once a stellarator is built and its magnetic geometry is fixed, further confinement improvement can be attained by identifying advanced operation scenarios in which so-called enhanced or high performance is achieved. From this perspective, enhancing our understanding of the phenomena present in high-performance scenarios of current experiments is highly relevant. In this overview, we will thoroughly discuss high-performance scenarios in the TJ-II stellarator in light of first-principles theory and simulations.

2. FIRST-PRINCIPLES MODELING OF HIGH-PERFORMANCE SCENARIOS

Access to high performance in stellarators has a long history. Some key milestones are the high-density H-mode plasmas obtained in W7-AS [6], the high T_i plasmas with internal transport barriers in LHD [7] or the pellet-fuelled enhanced confinement in W7-X [8]. All of them display a variety of high-performance signatures, including increased energy confinement time and stored energy, higher core temperature values, and largely suppressed turbulence and turbulent heat fluxes. While the specific conditions leading to enhanced performance vary across devices, they are generally associated to modifications of plasma parameters such as the density gradient of the bulk species, absolute density levels, or, in some LHD and W7-X discharges, also the introduction of a controlled amount of low-charge-state impurities.

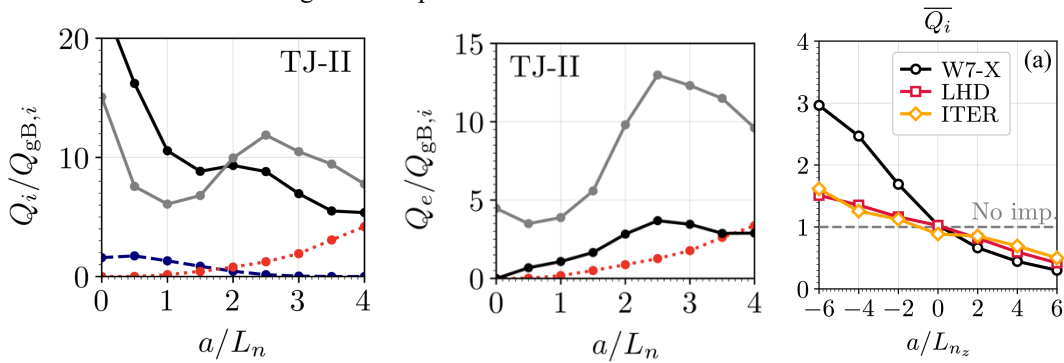


Figure 1: Turbulent ion (left) and electron (middle) heat fluxes obtained by means of nonlinear electrostatic gyrokinetic simulations with the code `stella` as a function of the normalized density gradient, a/L_n , for the TJ-II stellarator, considering normalized ion and electron temperature gradients $a/L_{T_i} = a/L_{T_e} = 3.0$ (gray), neglecting a/L_{T_e} (black), retaining a/L_n only (red) and a/L_{T_e} only (blue). On the right, main ion heat flux relative to its values in the absence of impurities as function of the impurity density gradient, considering C^{6+} and $Z_{\text{eff}} = 1.4$ for W7-X, LHD, and ITER. Figures from [9] and [11].

In this context, recent advances have been driven by first-principles theory and simulation. The role of the density gradient on microturbulence has been investigated by means of gyrokinetic simulations across several devices, showing a strong reduction of heat fluxes [9] (see figure 1, left and middle, for the turbulent ion and electron heat fluxes in the TJ-II stellarator). As for the density profile itself at the inner core, it has been to a large extent explained by the balance between inward and outward turbulent and neoclassical, respectively, convection terms [10]. Finally, it has also been numerically characterized the active role of impurities on regulating background

turbulence, enhancing or reducing, depending on the relative sign of the impurity and main ion density profiles, both fluctuations and heat fluxes [11] (see figure 1, right).

3. HIGH PERFORMANCE IN THE TJ-II STELLARATOR

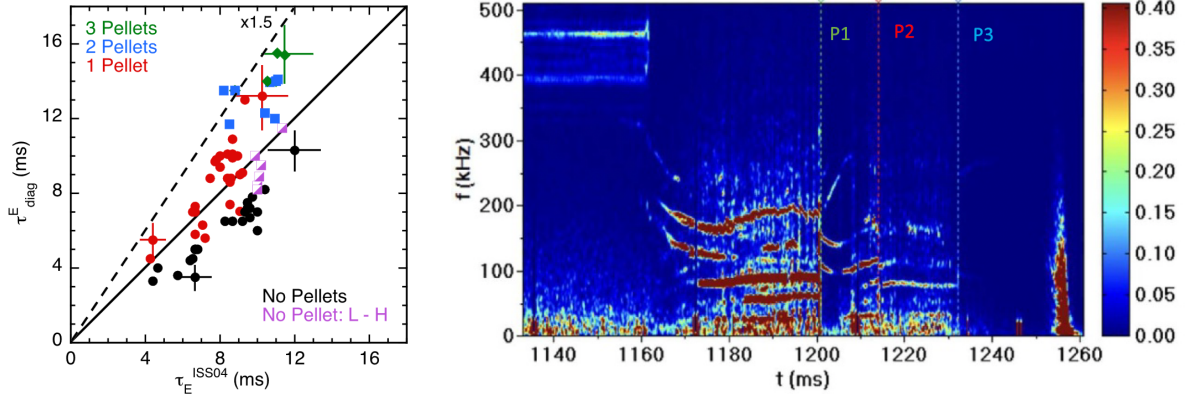


Figure 2: (Left) Energy confinement time in TJ-II is compared to the ISS04 scaling for high performance scenarios achieved by the injection of a different number of pellets. Baseline discharges and H mode scenarios are also included for reference. (Right) Fast-Fourier transform spectrogram measured by one HIBP system at $\rho = 0.5$ during TJ-II discharge #52582. Pellets are injected at three instants, indicated by vertical dashed lines, and followed but strong reduction of the fluctuation level. Figures from [15].

The medium-sized TJ-II stellarator represents a paradigmatic example of access to these high-performance scenarios, with multiple pathways documented throughout its extended operation. Some examples include L-H transition achieved through improved plasma-wall interaction obtained with Li-coating [12], and triggered by the suppression of turbulence associated to global sheared flows [13]. More recently, an improved regime has been achieved by means of pellet injection, closely resembling the equivalent pellet-fuelled high-performance plasmas in W7-X. As shown in figure 2 (left), this led to an improvement of the energy confinement time in TJ-II of a factor of up to 50%. This scenarios, presented in [14], have recently been expanded, and their experimental characterization has been improved [15]: the injection of multiple pellets has been considered; the observed effects have been compared for co- and counter-injection of NBI; the CXRS system has been recommissioned, enabling the measurement of ion temperature profiles; and density and electrostatic potential fluctuation measurements using Doppler reflectometry and the HIBP system have been added, see figure 2 (right). This experimental effort, combined with the numerical characterization of fundamental turbulence properties and their connection to particle and energy transport (see Section 2 of this synopsis), converges in time, providing a unique opportunity for code validation against experiments and a more accurate interpretation of the results.

4. SCOPE OF THIS WORK

With this spirit of validation and interpretation of experimental measurements, the present work undertakes a systematic characterization of transport in TJ-II with first-principles simulations. The results of these simulations are compared against available experimental measurements, including the evolution of confinement, fluctuation measurements, and particle and power transport coefficients through analyses similar to those carried out for W7-X [16]. Non-pellet-fueled scenarios, including co- and counter-NBI cases as well as baseline ECRH discharges, will also be discussed. Particular attention is given to the universality of the identified confinement improvement mechanisms, their relevance to understand enhance confinement regimes in W7-X and their extrapolation to reactor conditions.

REFERENCES: [1] C. D. Beidler et al., *Nature* 596, 221 (2021); [2] E. Sánchez et al., *Nucl. Fusion* 63, 066037 (2023); [3] J. M. García-Regaña et al. *Nucl. Fusion* 65, 016036 (2025); [4] A. G. Goodman et al. *Phys Rev. X* Energy 3, 023010 (2024); [5] P. Kim et al. *J. Plasma Phys.* 90 (2) 905900210 (2024); [6] K. McCormick et al., *Phys. Rev. Lett.* 89, 015001 (2002); [7] H. Takahashi et al., *Nucl. Fusion* 58, 106028 (2018); [8] S. Bozhenkov et al., *Nucl. Fusion* 60, 066011 (2020); [9] H. Thienpondt et al., *Nucl. Fusion* 65, 016062 (2025); [10] H. Thienpondt et al., *Phys. Rev. Res.* 5, L022053 (2023); [11] J. M. García-Regaña et al., *Phys. Rev. Lett.* 133, 105101 (2024); [12] J. Sánchez et al. *Nucl. Fusion* 49, 104018 (2009); [13] T. Estrada et al., *Plasma Phys. Control. Fusion* 51, 124015 (2009); [14] I. García-Cortés et al., *Phys. Plasmas* 30, 092303 (2023) and this conference; [15] K. J. McCarthy et al. *Nucl. Fusion* 64, 066019 (2024); [16] D. Carralero et al. *Plasma Phys. Control. Fusion* 64 044006 (2022).